

1            ***Deciphering inhibitory activity of flavonoids against tau protein***  
2 ***kinases: A coupled molecular docking and quantum chemical study***

3            Hassan Rasouli<sup>1\*</sup>, i<sup>2</sup>, Reza Yarani<sup>3</sup>, Ali Altıntaş<sup>4</sup>, Saber Ghafari Nikoo Jooneghani<sup>2, 5</sup>,  
4            Teodorico C. Ramalho<sup>6\*</sup>

5  
6            <https://doi.org/10.1080/07391102.2020.1814868>  
7

8  
9            1: National Institute of Genetic Engineering and Biotechnology (NIGEB), Tehran, Iran.

10            2: Department of Chemistry, Faculty of Science, Arak University, Arak, Iran.

11            3: TID Biology, Department of Clinical Research, Steno Diabetes Center Copenhagen, Denmark.

12            4: Novo Nordisk Foundation Center for Basic Metabolic Research, Faculty of Health & Medical  
13 Sciences, University of Copenhagen, Copenhagen, Denmark.

14            5: Quantum Chemistry Group, Department of Chemistry, Faculty of Sciences, Arak University,  
15 Arak, Iran.

16            6: Department of Chemistry, Federal University of Lavras, Brazil.

17  
18 \* Corresponding authors: [h3n.rasouli@gmail.com](mailto:h3n.rasouli@gmail.com) or [teodorico.ramalho@gmail.com](mailto:teodorico.ramalho@gmail.com)  
19

20            **Abstract**

21            Today, Alzheimer's disease (AD) is one of the most important neurodegenerative  
22 disorders that affected millions of people around the world. Hundreds of academic  
23 investigations highlighted the potential roles of natural metabolites in the cornerstone of AD  
24 prevention. Nevertheless, alkaloids are only metabolites that successfully showed promising  
25 clinical therapeutic effects on the prevention of AD. In this regard, other classes of plant  
26 metabolites such as flavonoids are also considered to be promising substances in the  
27 improvement of AD complications. The lack of data on molecular mode of action of  
28 flavonoids inside brain tissues, and their potential to transport across the blood-brain barrier,  
29 a physical hindrance between bloodstream and brain tissues, limited the large-scale  
30 application of these compounds for AD therapy programs. Herein, a coupled docking and  
31 quantum study was applied to determine the binding mode of flavonoids and three protein  
32 kinases involved in the pathogenesis of AD. The results suggested that all docked metabolites  
33 showed considerable binding affinity to interact with target receptors, but some compounds  
34 possessed higher binding energy values. Because docking simulation cannot entirely reveal  
35 the potential roles of ligand substructures in the interaction with target residues, quantum  
36 chemical analyses (QCAs) were performed to cover this drawback. Accordingly, QCAs  
37 determined that distribution of molecular orbitals have a pivotal function in the determination  
38 of the type of reaction between ligands and receptors; therefore, using such quantum  
39 chemical descriptors may correct the results of virtual docking outcomes to highlight  
40 promising backbones for further developments.

41  
42            **KEYWORDS:** Docking, Quantum calculations, Flavonoids, Kinase, Alzheimer.  
43  
44  
45  
46  
47  
48  
49  
50

51  
52  
53  
54  
55  
56  
57  
58  
59  
60  
61  
62  
63  
64  
65  
66  
67  
68

#### **ABBREVIATIONS:**

**AD:** Alzheimer’s disease; **A $\beta$ :** amyloid- $\beta$ ;  **$\tau$ :** tau; **ERK1/2:** extracellular-regulated kinase 1/2; **GSK-3 $\beta$ :** glycogen synthase kinase-3 $\beta$ ; **Cdk5:** cyclin-dependent kinase 5; **PKC:** protein kinase C alpha; **PKB/AKT:** protein kinase B; **PKA:** protein kinase A; **DYRK1A:** dual-specificity tyrosine-[Y]-phosphorylation-regulated kinase 1A; **CK1d:** casein kinase 1 delta; **MAPK10:** Mitogen-activated protein kinase 10; **JNK3:** c-Jun N-terminal kinase 3; **P38:** p38 delta kinase; **BBB:** the blood-brain barrier; **FMO:** frontier molecular orbitals; **HOMO:** highest occupied molecular orbital; **LUMO:** lowest occupied molecular orbital; **FERMO:** Frontier Effective-for-Reaction Molecular Orbital; **HSAB:** hard-soft acid-base; **KS:** Kohen-Sham; **HF:** Hartree–Fock; **DFT:** Density functional theory; **C3G:** Cyaniding-3-O-glucoside; **M3G:** malvidin-3-O-glucoside; **AChE:** acetylcholinesterase; **MEP:** Molecular electrostatic potential; **QM:** quantum mechanics; **HSAB:** Pearson’s hard-soft, acid and base; **CNS:** Central nervous system.

#### **1. INTRODUCTION**

“*I have lost myself*” has sorrowfully expressed by *Auguste Deter*, the first patient diagnosed with AD (Maurer *et al.*, 1997), and that was a story to set off research on this brain disease. Simply, AD targets innermost tissues and/or signaling pathways of the brain, consequently leading to cognitive dysfunction, dementia, depression, and degeneration of brain cells (Dubois *et al.*, 2018, McDade and Bateman, 2017). Although the molecular basis of AD pathogenesis is not comprehensively understood, the accumulating body of evidence suggests that the disease mainly causes damage to brain cerebral cortex and hippocampus regions, by which the injuries gradually distend to other parts of the brain (Dubois *et al.*, 2018).

The hyper-phosphorylation of  $\tau$  protein, the aggregation of A $\beta$  fibrils, and enhanced oxidative stress are three characteristic hallmarks of AD affected brains (Association, 2018, Maurer *et al.*, 1997). Microtubule-associated  $\tau$  protein is widely expressed in neurons, involved in the stabilization of neuronal scaffold, has structurally four domains to interact with related cellular targets, and is phosphorylated at 85 important amino acid sites (Martin *et al.*, 2013). Functionally, some transferase enzymes are responsible to substitute a phosphate moiety from energy donor substances such as ATP and GTP to specific biomolecules or substrates, which are involved in the phosphorylation of  $\tau$  protein (Martin *et al.*, 2013). Various types of  $\tau$  protein kinases have been identified and their function, structure, regulation and involvement in neurodegenerative processes linked to Alzheimer pathology are well described (Chico *et al.*, 2009). In this regard, protein kinases including ERK1/2 (Sun and Nan, 2017), GSK-3 $\beta$  (Lescot *et al.*, 2005), Cdk5 (Liu *et al.*, 2016), PKC (Clark *et al.*, 1991), PKB/AKT (Griffin *et al.*, 2005), PKA, DYRK1A, CK1d, MAPK10, JNK3 and p38 (Alvarez *et al.*, 1999, Dolan and Johnson, 2010, Schwab *et al.*, 2000) are deemed to be dysregulated and involved in the hyperphosphorylation of  $\tau$  protein .

Some factors including low bioavailability, ability to transport across BBB (Sweeney *et al.*, 2018), and possible side effects of natural products in brain tissues are limited their widespread application in AD therapy horizons (Scotti and Scotti, 2018). Up to now, among natural products, alkaloids are only pioneer metabolites in the cornerstone of human diseases prevention (Ng *et al.*, 2015, Rasouli *et al.*, 2020). Additionally, several flavonoids have also transported across the BBB to interact with a variety of brain proteins and signaling pathways

100 (Faria *et al.*, 2014, Yang *et al.*, 2014), but their molecular mode of action remained unknown  
101 (Faria *et al.*, 2012).

102 Studies demonstrate that data obtained from docking results might determine the physical  
103 interaction of ligands-receptors mediated by sharing electrons from each side of reaction  
104 (Glaab, 2015, Rasouli *et al.*, 2017). In such a situation, determining the portion of each ligand  
105 moiety or residue side chain in the debuting of expected interactions is difficult or not  
106 fundamentally possible (Rasouli *et al.*, 2017). On the other hand, current docking scoring  
107 functions could not effectively highlight the priority of ligands atoms or active site residues in  
108 the first encounter of ligand-receptor (Klebe, 2006).

109 Over the past decades, molecular docking simulation has adequately been helping  
110 researchers to know how ligands correctly interact with their targets (Rasouli *et al.*, 2017).  
111 Despite its popularity, the molecular docking method presently suffered from several  
112 limitations including the lack of qualitative databases for validating the outcomes, the  
113 presence of false-positive results, and the obscurity linked to docking scoring mathematical  
114 functions (Glaab, 2015, Klebe, 2006). To solve these problems, studies suggested that  
115 docking results alone are not reliable, and coupling these outcomes with advanced  
116 computational methods such as molecular dynamics simulation and quantum chemical  
117 analyses might partly overcome these concerns and improve fidelity and accuracy of docking  
118 outputs (Ghazvini *et al.*, 2018, Raha and Merz, 2004, Rasouli *et al.*, 2017, Yuriev and  
119 Ramsland, 2013). To evaluate this possibility, quantum chemical calculations and traditional  
120 docking simulation were coupled for different targets and the results are as the follows.

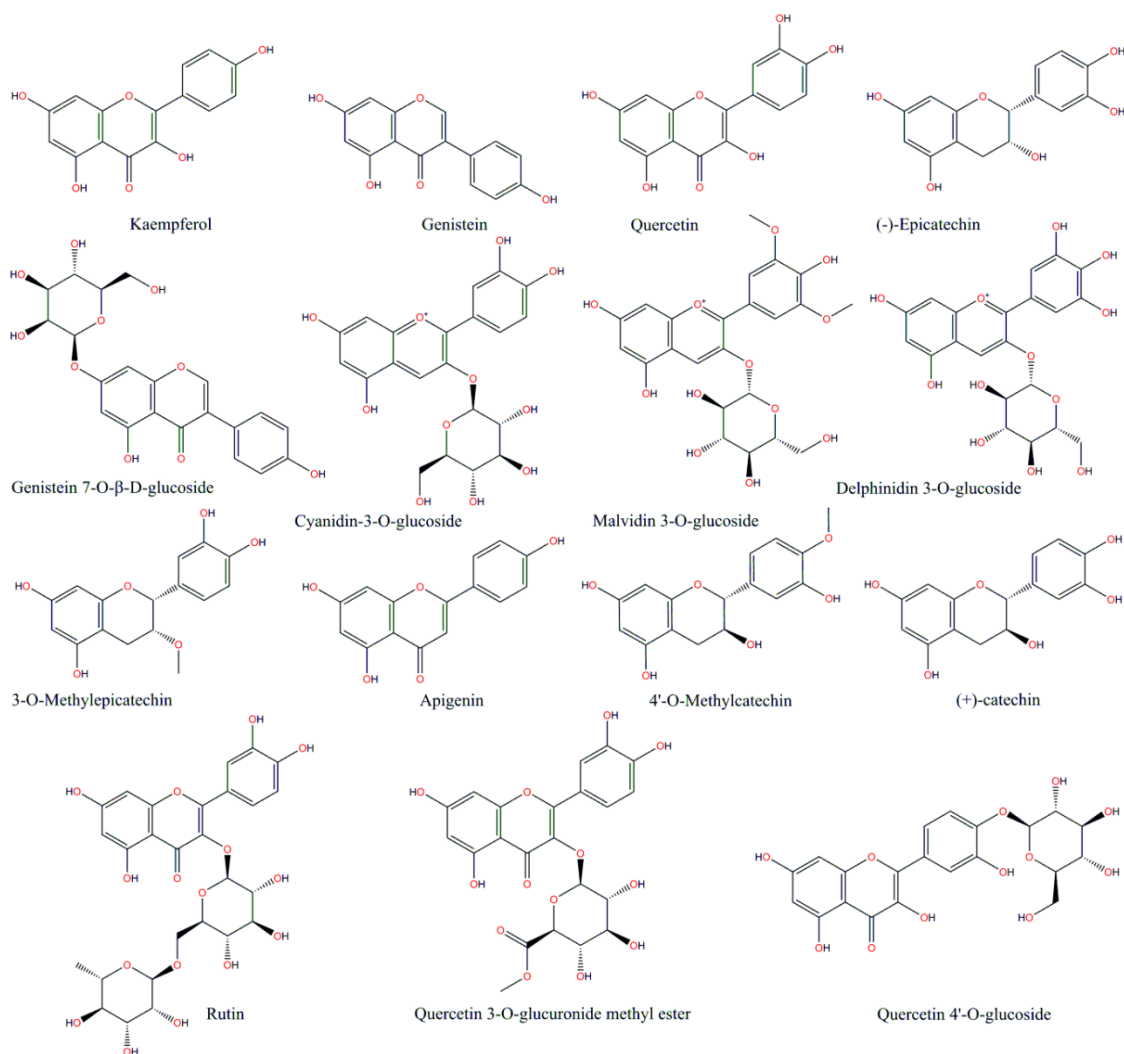
121

## 122 **2. COMPUTATIONAL DETAILS**

### 123 **2.1. LIGAND PREPARATION**

124 Because of limitations with measuring flavonoids mode of action within the brain tissues,  
125 the fingerprint of flavonoids appearance in the central nervous system has only been  
126 reported by limited number of studies (Faria *et al.*, 2012, Faria *et al.*, 2014, Faria *et al.*, 2010,  
127 Ferri *et al.*, 2015, Yang *et al.*, 2014). Accordingly, 15 flavonoid metabolites with potential to  
128 transport across the BBB were chosen as input ligands for computational analyses (**Fig.1**).

129



130

131 **Fig.1.** The 2D illustration of selected flavonoids for docking and quantum analyses.

132

## 133 2.2. RECEPTOR PREPARATION AND MOLECULAR DOCKING

134 The 3D crystallographic structures of Cdk5-p25 (PDB ID: 3O0G (Ahn *et al.*, 2005)),  
 135 GSK3β (PDB ID: 1J1C (Aoki *et al.*, 2004)) and CK1δ (PDB ID: 3UYT (Long *et al.*, 2012))  
 136 as target kinases were taken up from PDB database (<https://www.rcsb.org/>). The importance  
 137 of these receptors in the pathogenesis of AD has been formerly reported (Adler *et al.*, 2019,  
 138 Llorens-Marín *et al.*, 2014, Wilkaniec *et al.*, 2016, Wilkaniec *et al.*, 2018). First, water  
 139 molecules and other heteroatoms were removed from the structure of obtained receptors.  
 140 MODELLER version 9.22 software (<https://salilab.org/modeller/>) was applied to correct the  
 141 conformation of some missing residues. Next, 10 ns molecular dynamic simulation using  
 142 Gromacs version 5.0.1 tool ([www.gromacs.org](http://www.gromacs.org)) was recruited to prepare the initial structure  
 143 of amended receptors.

144 Molecular blind docking using AutoDock 4.2.6 (Trott and Olson, 2010) was carried out,  
 145 and the missing hydrogens and Gasteiger/Kollman charges were assigned to the prepared  
 146 system during performing docking analysis. The map of standard grid boxes for molecular  
 147 docking was generated using AutoGrid 4.2.6 in which the size of grid box was 50 × 50 × 50  
 148 Å (x, y, and z) points and grid-point spacing of 0.375 Å, respectively. The number of  
 149 independent docking runs performed for each docking simulation was set to 200 with

150 25,000,000 energy evaluations for each run. The Lamarckian genetic algorithm was also used  
151 for performing energy minimization and optimization during the time of molecular docking  
152 simulation. GaussView 3.0 tool (Frisch *et al.*, 2004) was applied to prepare graphical  
153 illustration of Gaussian outputs.

154

### 155 **2.3. QUANTUM ANALYSES**

156 First, TAO package (Tao and Schlegel, 2010) was recruited to isolate a sphere with 5Å  
157 radius around each studied active site to determine the electronic structures of ligand-active  
158 site complexes. All included residues in this sphere were evaluated for their electronic  
159 structures. Protoss web-server (Bietz *et al.*, 2014) was applied to protonate the isolated  
160 spheres, and Gaussian 03 (Frisch *et al.*, 2004) was used for further single point calculations at  
161 two methods including *HF/6-31G(d)* and *B3LYP/6-31G(d)*. The SCPA method was also  
162 employed to validate the contribution of molecular orbitals in each residue and/or ligand  
163 substructures using Multiwfn software (Lu and Chen, 2012). In this study, the compounds  
164 comprised both types of pure and conjugated flavonoids (methylated and glycosidic forms).  
165 Three fragments including sugar moiety, two rings of flavonoids backbone (including A and  
166 C rings) and B-ring alone were chosen as input segments for quantum chemical analysis.

167

## 168 **3. RESULTS**

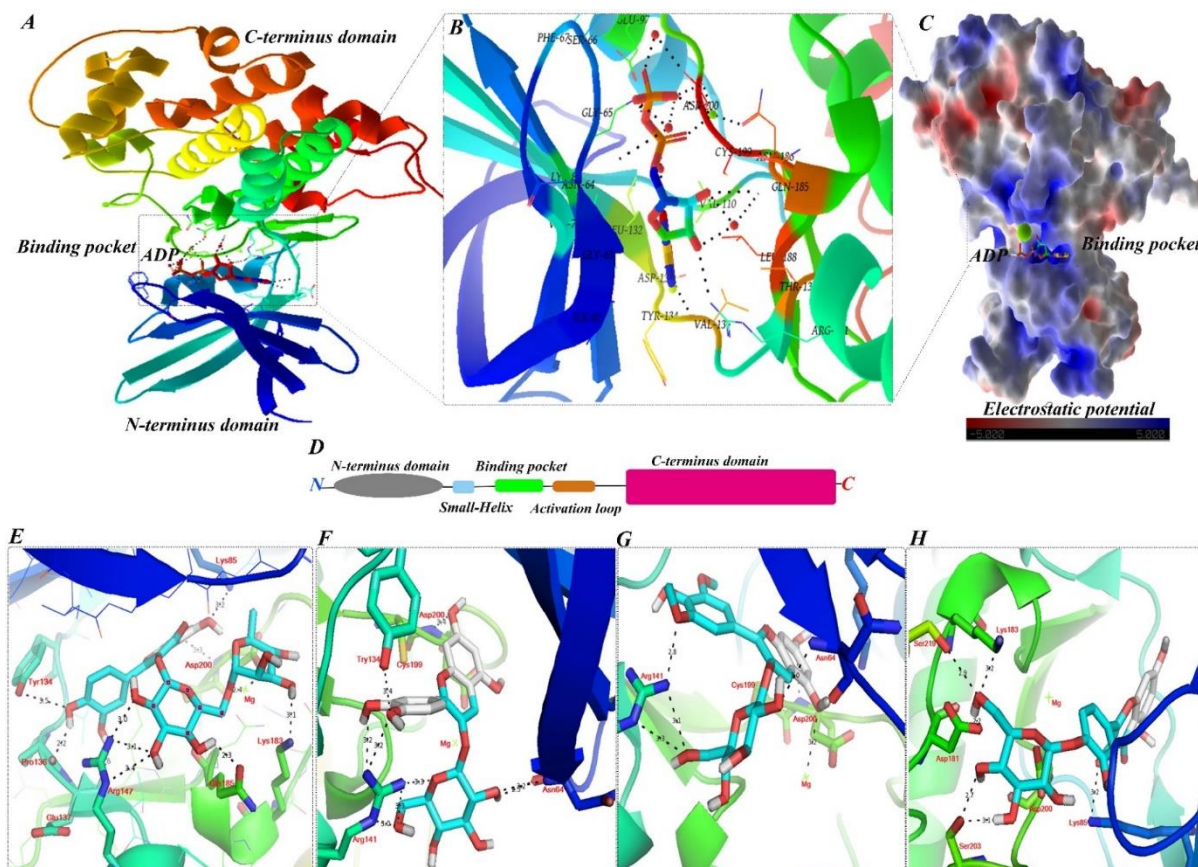
### 169 **3.1. INTERACTION WITH GSK3β**

170 According to docking simulation results for GSK3β enzyme, all ligands were able to  
171 interact with the active site of this receptor by possessing binding energies ranging from -7.1  
172 to -10.42 kcal·mol<sup>-1</sup>. In comparison to crystallographic data of GSK3β active site (Aoki *et al.*,  
173 2004), rutin, cyanidin-3-O-glucoside, malvidin-3-O-glucoside and quercetin-4'-O-glucoside  
174 posed nearby its catalytic and binding residues (**Fig. 2**). The calculated binding energies for  
175 these compounds were -10.42, -9.76, -9.30 and -9.17 kcal·mol<sup>-1</sup>, respectively. Indeed, other  
176 compounds were also interacted with this active site by gaining lower docking binding  
177 energies. Accordingly, two oxygen atoms from OH7 of rutin A-ring and its sugar moiety  
178 (rutinose disaccharide) have formed hydrogen bonds with NE and NHE2 atoms of Arg<sup>141</sup>.  
179 Another oxygen atom from OH group of 4' position of rutin B-ring also interacted with the  
180 OH of Tyr<sup>134</sup> to create a hydrogen bond. The O atom of Pro<sup>136</sup> also interacted with the OH  
181 group of 4'-position of rutin B-ring. Similarly, the backbone O atom of Glu<sup>137</sup> interacted with  
182 the hydroxyl group of 3'-position of rutin B-ring. The NZ of Lys<sup>85</sup> formed a hydrogen bond  
183 with the backbone OH group of 5-position of rutin A-ring.

184 The backbone N atom of Asp<sup>200</sup> created a hydrogen bond with another oxygen atom  
185 of rutin. Oxygen atoms of rutin sugar were also interacted with the metal group (*i.e.*  
186 magnesium). The O atom of Gln<sup>185</sup> also interacted with the OH4" group of rutin sugar moiety  
187 through H-donor interaction. The oxygen atom of rutinose moiety also formed a hydrogen  
188 bond with the NZ atom of Lys<sup>183</sup>. The average distance of H-bonds between rutin and GSK3β  
189 was ~3.1Å, followed by residue-ligand atom binding energy equals to -1.8 kcal·mol<sup>-1</sup>.  
190 Similar interactions were also observed for cyanidin-3-O-glucoside. The backbone N atom of  
191 Asn<sup>64</sup> formed a hydrogen bond with the sugar OH group of cyaniding-3-O-glucoside. Also,  
192 the O atom of this residue interacted with the sugar unit of cyanidin-3-O-glucoside. The N  
193 atom of Asp<sup>200</sup> constructed a hydrogen bond with OH7 group of A-ring of this compound.  
194 Also, Tyr<sup>134</sup>, Arg<sup>141</sup>, and Cys<sup>199</sup> were other residues in this active site that actively  
195 participated in the interaction of this cavity with its docked ligand.

196 The anthocyanin malvidin-3-O-glucoside was another top docked compound that was  
197 located in the active site of GSK3β. As depicted in **Fig. 2**, this anthocyanin interacted with

198 active site residues to form powerful hydrogen bonds. In addition to the above-mentioned  
 199 metabolites, quercetin-4'-O-glucoside formed hydrogen bonds with GSK3 $\beta$  residues  
 200 including Lys<sup>85</sup>, Asp<sup>181</sup>, Lys<sup>183</sup>, Asp<sup>200</sup>, Ser<sup>203</sup>, and Ser<sup>219</sup>, respectively. The average distance  
 201 of created H-bonds per residue for quercetin-4'-O-glucoside/GSK3 $\beta$  active site residues was  
 202  $\sim 2.90$  Å followed by residue-atom interaction energy equals to  $-1.5$  kcal $\cdot$ mol<sup>-1</sup>.  
 203



204  
 205 **Fig. 2.** Docking results for GSK3 $\beta$ . The structure of GSK3 $\beta$  (PDB id: 1J1C(Aoki *et al.*,  
 206 2004)) in complex with ADP molecule (A), its active site binding and catalytic residues (B)  
 207 and Poisson-Boltzmann surface electrostatic potential (C) are shown in this illustration. In  
 208 panel (C) red color represents negative surface charge, blue shows positive charges and  
 209 neutral regions is shown in white color. As depicted in panel (D), protein kinases have unique  
 210 structural features including N- and C-terminus domains, small helix, binding pocket and  
 211 activation loop in which possessed highly conserved catalytic residues (Aoki *et al.*, 2004,  
 212 Chico *et al.*, 2009). Biochemically, conformational changes of N or C terminus domains  
 213 would determine the activity protein kinases (Kokubo *et al.*, 2013). The binding mode of (E)  
 214 rutin; (F) cyanidin-3-O-glucoside; (G) malvidin-3-O-glucoside and (H) quercetin-4'-O-  
 215 glucoside are also shown in the bottom of the illustration. In addition to the formation of H-  
 216 bonds, compounds E and G were also interacted with Mg ion in this active site.  
 217

### 218 3.2. INTERACTION WITH CDK5-p25

219 The docking outcomes for Cdk5-p25 enzyme and selected flavonoids showed that these  
 220 compounds have also potentially interacted with the active site residues of this enzyme.  
 221 Rutin, delphinidin-3-O-glucoside, malvidin-3-O-glucoside and quercetin-4'-O-glucoside  
 222 exhibited potent docking binding energies. The binding energy values of these top  
 223



224 compounds were -10.0, -9.89, -8.10 and -7.02 kcal·mol<sup>-1</sup>, followed by the average H-bond  
225 distance of ~2.1 Å, and residue-atom interaction energy equals to -2 kcal·mol<sup>-1</sup>, respectively.

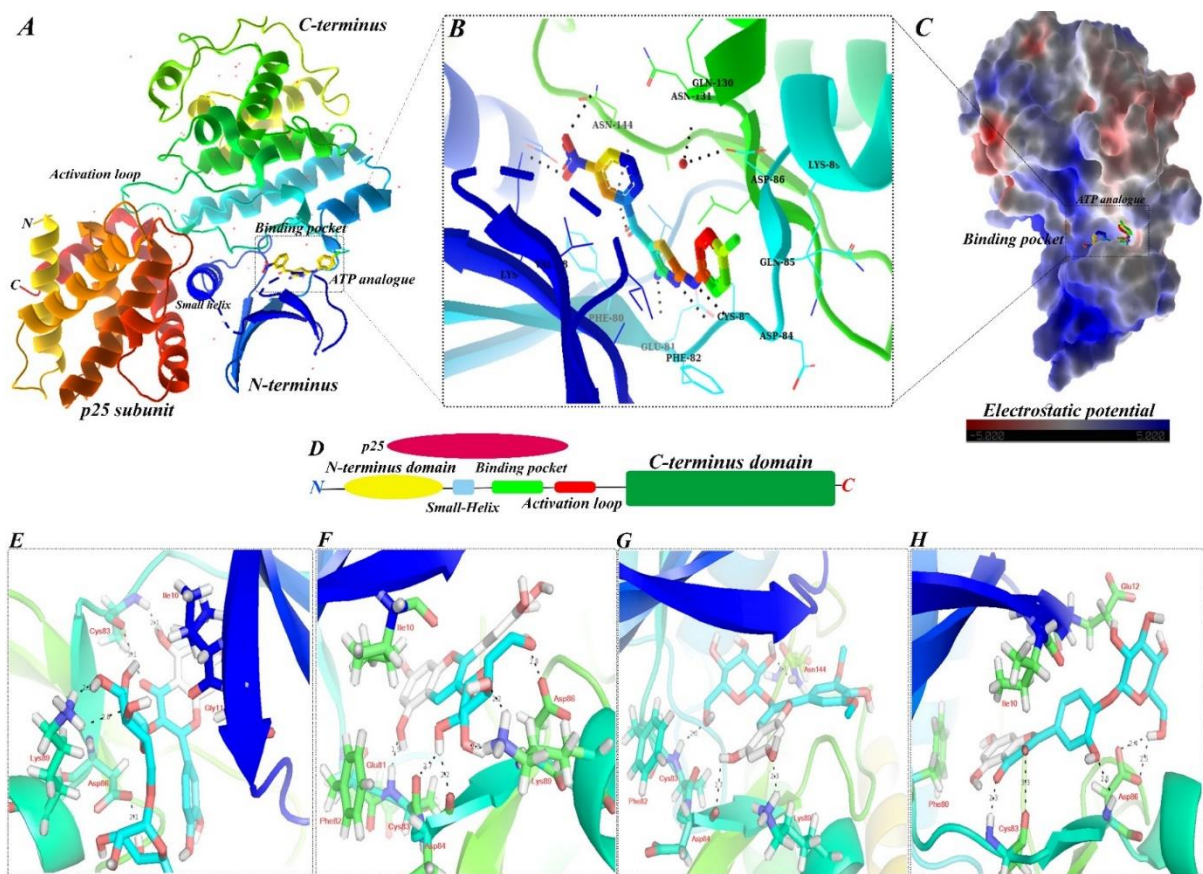
226 Binding mode analysis of top docked compounds showed that these ligands formed both  
227 H-donor and H-acceptor interactions within this active site. Crystallographic data indicated  
228 that several residues including Leu<sup>10</sup>, Glu<sup>12</sup>, Val<sup>18</sup>, Phe<sup>80</sup>, Glu<sup>81</sup>, Phe<sup>82</sup>, Cys<sup>83</sup>, Asp<sup>84</sup>, Glu<sup>85</sup>,  
229 Asp<sup>86</sup>, Leu<sup>133</sup> and Asn<sup>144</sup> (or Asp<sup>144</sup>) were participated in the formation of H-bonds or other  
230 non-covalent interactions with the backbone of small molecule inhibitors (Ahn *et al.*, 2005).  
231 The docking results for studied compounds showed that docked flavonoids could easily enter  
232 the cavity Cdk5-p25 active site and formed several H-bonds with its catalytic and binding  
233 amino acids.

234 Interestingly, the OH7 group of quercetin-4'-O-glucoside constructed a non-covalent H- $\pi$   
235 interaction with benzyl side chain of Phe<sup>80</sup> residue. The formed hydrogen bonds between the  
236 docked compounds and Cdk5-p25 active site residues indicated that these ligands have the  
237 potential to facilitate the disruption of its normal biological activity (Ahn *et al.*, 2005). In this  
238 regard, recent enzymatic investigation indicated that some flavonoid-based inhibitors of  
239 Cdk5-p25 tightly interacted with its catalytic residues and possessed IC<sub>50</sub> value equal to  
240 4.81  $\mu$ M, respectively (Shrestha *et al.*, 2013).

241 Studies showed that the entrance of ligands into the active site cavity is simultaneously  
242 associated with the possible changes in active site cavity shape and function (Ghazvini *et al.*,  
243 2018, Rasouli *et al.*, 2017). The essence of active site residues (acidic, hydrophobic, *etc.*) and  
244 chemical structure of inhibitors might function as two determinant factors to affect the  
245 possible interaction of ligands and receptors (Rasouli *et al.*, 2018). In comparison to docking  
246 outcomes of GSK3 $\beta$ , the calculated docking energies were not greater, and the number of  
247 formed H-bonds were also decreased (**Fig. 3**). This may indicate that the studied metabolites  
248 might have a dose-dependent inhibitory profile for this enzyme *in vitro* or *in vivo*.

249

250



251

252

253 **Fig. 3.** Docking results for Cdk5-p25 (PDB id: 3O0G). Panels (A) the conformational  
 254 arrangement of Cdk5-p25 in complex with its inhibitor; (B) illustration of its critical active  
 255 site amino acids; (C) electrostatic surface potential and (D) simplified view of Cdk5-p25  
 256 structure. P25 subunit regulates the activation of this enzyme and without this fragment  
 257 Cdk5-p25 cannot handle its molecular functions (Tarricone *et al.*, 2001). Top docked ligands  
 258 including (E) rutin; (F) delphinidin-3-O-glucoside; (G) malvidin-3-O-glucoside and (H)  
 259 quercetin-4'-O-glucoside are shown the bottom sections of this illustration.

260

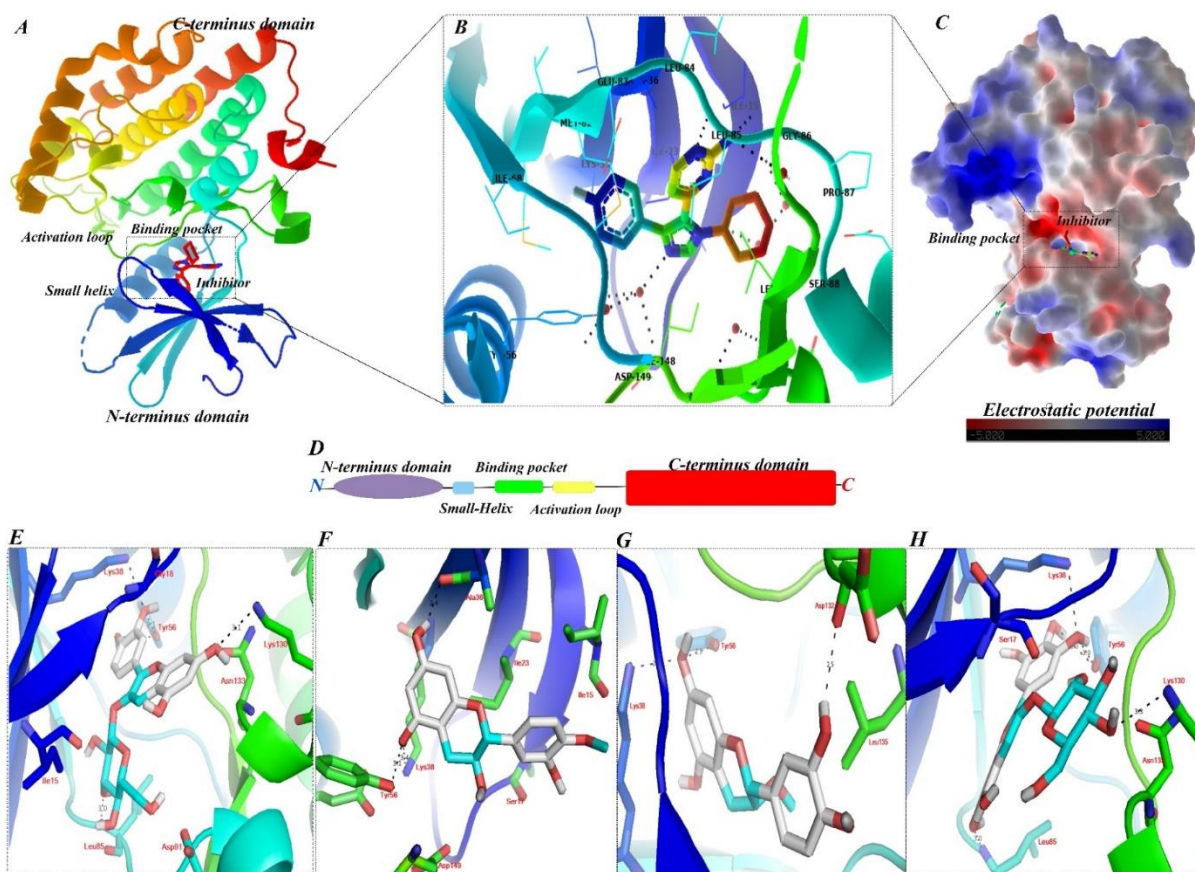
### 261 3.3. INTERACTION WITH CK1δ

262 The detailed information on most important residues of this active site formerly discussed  
 263 (Long *et al.*, 2012). Docking results for CK1δ enzyme displayed that four metabolites  
 264 including cyaniding-3-O-glucoside, 4'-methylcatechin, 3-O-methylepicatechin and  
 265 delphinidin-3-O-glucoside were tightly bound to the active site cavity of CK1δ through  
 266 forming covalent and non-covalent bridges (**Fig. 4**). The calculated binding energies for top  
 267 docked compounds were -8.11, -8.0, -7.30 and -7.0 kcal·mol<sup>-1</sup>, respectively. Both types of H-  
 268 acceptor and H-donor interactions were observed between ligands atoms and active site  
 269 amino acids. Additionally, CD1 atom of Ile<sup>23</sup> formed a non-covalent H-π interaction with A-  
 270 ring of 4'-methylcatechin. The docking results demonstrate that flavonoids compounds have  
 271 lower binding affinities for this receptor in comparison to GSK3β and Cdk5-p25.

272 The size of active site cavity, molecular weights and chemical structures of docked ligands  
 273 and tendency of ligands to interact with this active may be considered as potential factors to  
 274 inhibit this enzyme. However, the construction of H-bonding and other types of chemical  
 275 interactions between flavonoids backbone atoms and CK1δ active site amino acids including



276 Ser<sup>11</sup>, Ile<sup>15</sup>, Ile<sup>23</sup>, Lys<sup>38</sup>, Leu<sup>85</sup>, Asp<sup>91</sup>, Tyr<sup>65</sup>, Lys<sup>130</sup>, Asp<sup>132</sup> and Asn<sup>133</sup> residues demonstrated  
 277 that this enzyme is one the possible targets flavonoids metabolites can interact with its active  
 278 site after entrance the CNS environment.  
 279



280  
 281 **Fig. 4.** Docking results for CK1δ. Sections A-D depicted structural features of CK1δ  
 282 enzyme (PDB id: 3UYT (Long et al., 2012)). The binding mode of (E) cyaniding-3-O-  
 283 glucoside; (F) 4'-methylcatechin; (G) 3-O-methylepicatechin and (H) delphinidin-3-O-  
 284 glucoside are shown in the bottom of this illustration.  
 285

286 Apigenin, kaempferol, genistein and quercetin accordingly displayed similar docking  
 287 binding affinity energies against kinases. With binding energies of  $-6.0 \text{ kcal}\cdot\text{mol}^{-1}$ , followed  
 288 by the average H-bond distance of  $2.1 \text{ \AA}$ , their docking almost showed similar affinities  
 289 during docking simulations. Additionally, (-)-epicatechin and (+)-catechin showed acceptable  
 290 binding energy values for GSK3β ( $-8.01$  and  $-7.30 \text{ kcal}\cdot\text{mol}^{-1}$ ) and Cdk5-p25 ( $-6.5$  and  $-5.0$   
 291  $\text{kcal}\cdot\text{mol}^{-1}$ ) active sties. Quercetin 3-O-glucuronide methyl ester and genistein 7-O-β  
 292 glucoside also showed similar binding energies for GSK3β ( $-5.5 \text{ kcal}\cdot\text{mol}^{-1}$ ) and CK1δ ( $-5.0$   
 293  $\text{kcal}\cdot\text{mol}^{-1}$ ) receptors. In summary, all compounds could interact with catalytic residues of  
 294 target active sites, and it seems the variability of binding energies is related to chemical  
 295 structure of these compounds and tendency of active site residues to participate in the  
 296 occurred interactions.

297 In the following sections, we will show how distribution of molecular orbitals among  
 298 ligands backbone fragments or active site residues might provide valuable information on the  
 299 effectiveness of ligand-receptor interactions.  
 300  
 301

302  
303

### 3.4. QUANTUM RESULTS

304 According to quantum chemical results, the considered fragments including A/C scaffold,  
305 B-ring and sugar moiety unraveled different functions in the structure of studied ligands.  
306 Additionally, active site residues also shared similar behaviors, showing a specific pattern of  
307 molecular orbital distribution in their structure. By considering the isolated 5Å radius spheres  
308 from each active site, the quantum results suggested that each residue has a specific  
309 contribution in the distribution of molecular orbital levels. In both methods, considerable  
310 changes of MOs have been observed for ligand-receptor complexes and free structures  
311 (*Suppl. File S1- Table 1 to 5-1*). Indeed, based upon the chemical backbone of active site  
312 residues variable contributions have been found for studied active site amino acids (*Suppl.*  
313 *Fig. A1*).  
314

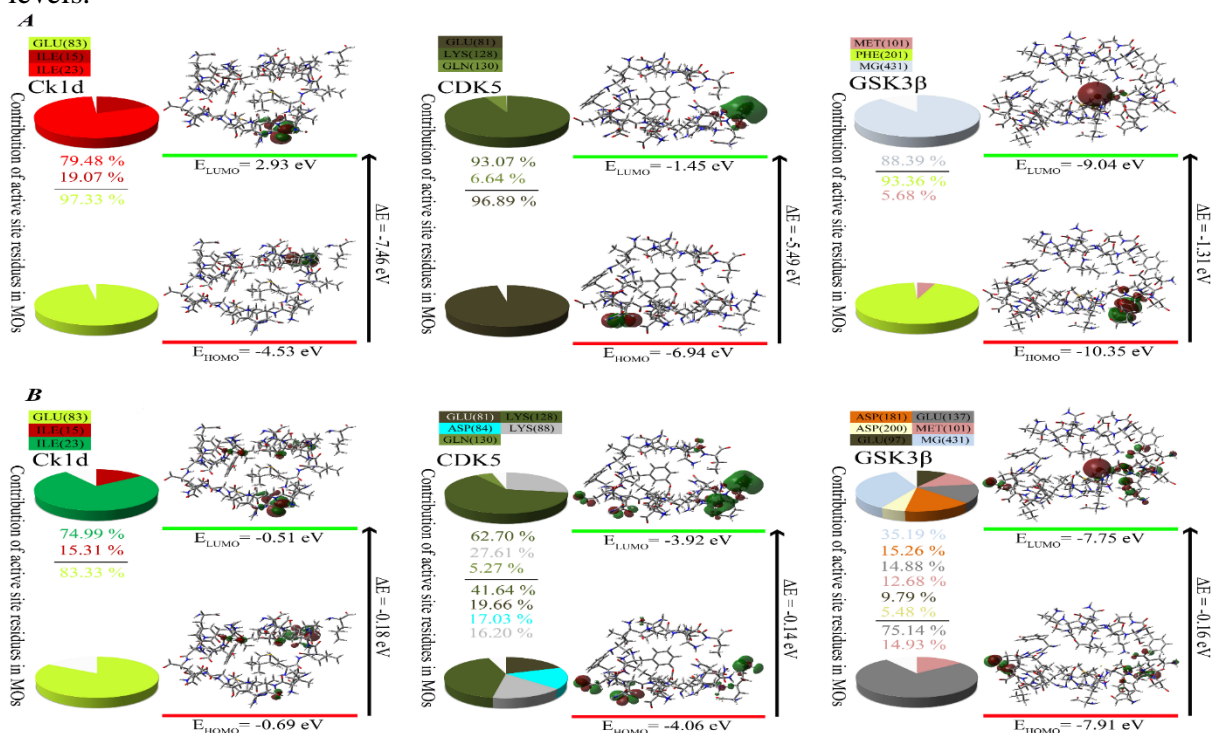
315 This finding significantly supports our understanding of the primary roles of LUMO and  
316 higher LUMO orbitals to address the participation of active site residues to interact with  
317 ligands and/or their substructures in the ligand-receptor complex. Fukui *et al.* (Fukui *et al.*,  
318 1954, Fukui *et al.*, 1952) applied the FMO theory to predict the process of chemical  
319 reactions, and this approach has clearly changed chemical views to understand the basic  
320 essence of chemical reactions and associated interactions. Hoffmann and Woodward  
321 (Hoffmann and Woodward, 1965, Hoffmann and Woodward, 1968) developed the FMO  
322 theory to highlight the critical roles of orbital symmetries in this concept. To overcome  
323 limitations with the gap between HOMO and LUMO orbitals, researchers have applied the  
324 FERMO concept (da Silva *et al.*, 2006) to predict the chemical behavior of ligands precisely.

325 According to FERMO theory, the chemical action of ligands in the first encounter with the  
326 receptors was determined by the shape and distribution of MOs (Silva *et al.*, 2006).  
327 Therefore, there is a possibility for ligands to possess various FERMOs to interact with the  
328 receptor active site residues specifically. As a result, a FERMO can be a HOMO orbital or  
329 other frontier orbitals (Silva *et al.*, 2006). Furthermore, the behavior of active site residues  
330 (both catalytic and binding amino acids) is a way to interpret the concept of hardness and  
331 softness, thus, the involvement of different substructures will be considered as FERMO  
332 (donor) and LUMO or higher LUMO (acceptor). Similarly, Klopman recruited a new concept  
333 called the charge and/or frontier-controlled reactions (Klopman, 1968) by considering  
334 Pearson's HSAB concept (Pearson, 1963).

335 Accordingly, when  $E_{gap}$  of FERMO (donor) and/or higher LUMO (acceptor) possesses a  
336 higher value; consequently, the reaction is charge controlled, and such condition describes the  
337 nature of hard-hard interactions (Pearson, 1963). Similarly, smaller amounts of this value  
338 predicted the frontier-controlled reaction and soft-soft interaction (Klopman, 1968, Pearson,  
339 1963). Considerably, much excitement generated from KS and HF molecular orbitals that  
340 showed similar behaviors to explain FERMO and LUMO in different datasets (some different  
341 behaviors for these molecular orbitals also reported) (da Silva *et al.*, 2006, Maksić and  
342 Vianello, 2006, Silva *et al.*, 2006).

343 The main reason for this phenomenon might be related to the intrinsic weakness of the KS  
344 molecular orbitals which will affect the effectiveness of outcomes. Knowing this issue helps  
345 us to apply both HF and DFT (B3LYP) methods to calculate molecular orbitals. Because of  
346 the higher accuracy of HF molecular orbitals compared to practical results (Ramalho *et al.*,  
347 2003), both HF and B3LYP results were also used to interpret quantum chemical outcomes.  
348 Meanwhile, the role of each active site residue in the expected interactions was also surveyed  
349 to find their best contribution with molecular orbitals. As depicted in *Fig.5*, the studied active  
350 site residues displayed a variable distribution in behavior, shape and rate of  $\Delta E_{gap}$  HOMO and

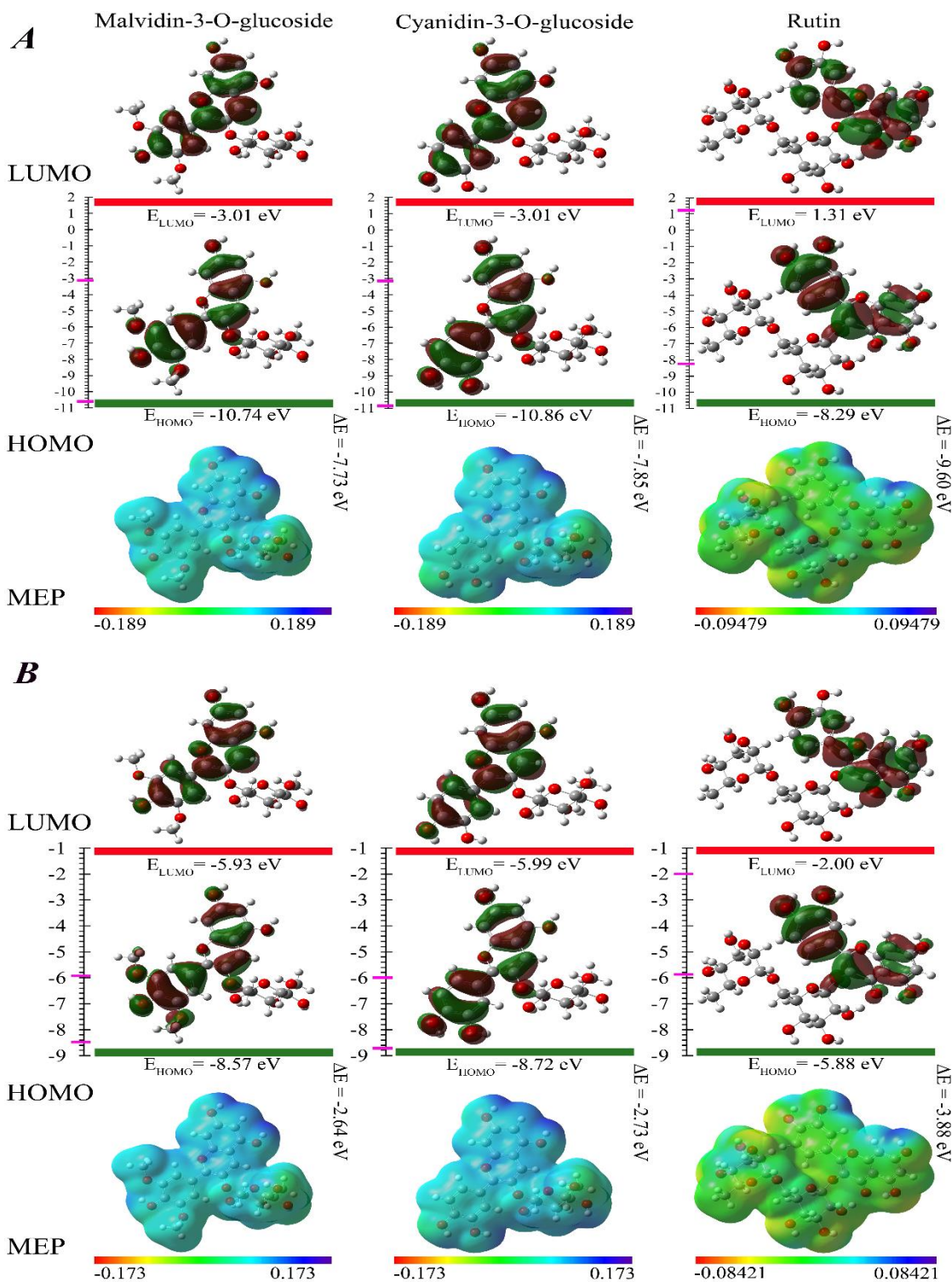
351 LUMO orbitals based on distribution's map of molecular orbitals in HOMO and LUMO  
 352 levels.



353  
 354 **Fig.5.** The participation of active site residues in MOs at (A) HF and (B) B3LYP methods.  
 355 As shown, target residues showed a considerable role in the distribution of molecular frontier  
 356 orbitals. These results indicate that simultaneous application of HF/B3LYP methods is a  
 357 reliable approach to generate high-quality quantum chemical outcomes. In both methods, Mg  
 358 ion of GSK3β active site contributed to the sharing of MOs within the active site.  
 359 Intriguingly, this ion formed strong H-bonds with some of docked flavonoids and these  
 360 calculations proved its critical role herein. The variability of active site residues contributions  
 361 speculated that the functionality of each active site is depending on the participation of these  
 362 residues to interact with nearby ligands. Indeed, numerical values of  $\Delta E_{gap}$  for residual  
 363 contribution to the dissemination of MOs are different at each method.

364  
 365 According to the calculated values of  $\Delta E_{gap}$  HOMO and LUMO orbitals (at both methods),  
 366 the studied fragments demonstrated a considerable variation in the first encounter of the  
 367 ligand-receptor complex for sharing their role in the distribution of MOs (Fig.6). The  
 368 distribution of MOs in the structure of each ligand depends on the substituted chemical  
 369 groups attached to the ligand skeleton, playing a pivotal role in the interaction of ligands with  
 370 favorable receptor amino acids in coincidence with the shared molecular orbitals of active  
 371 site residues.





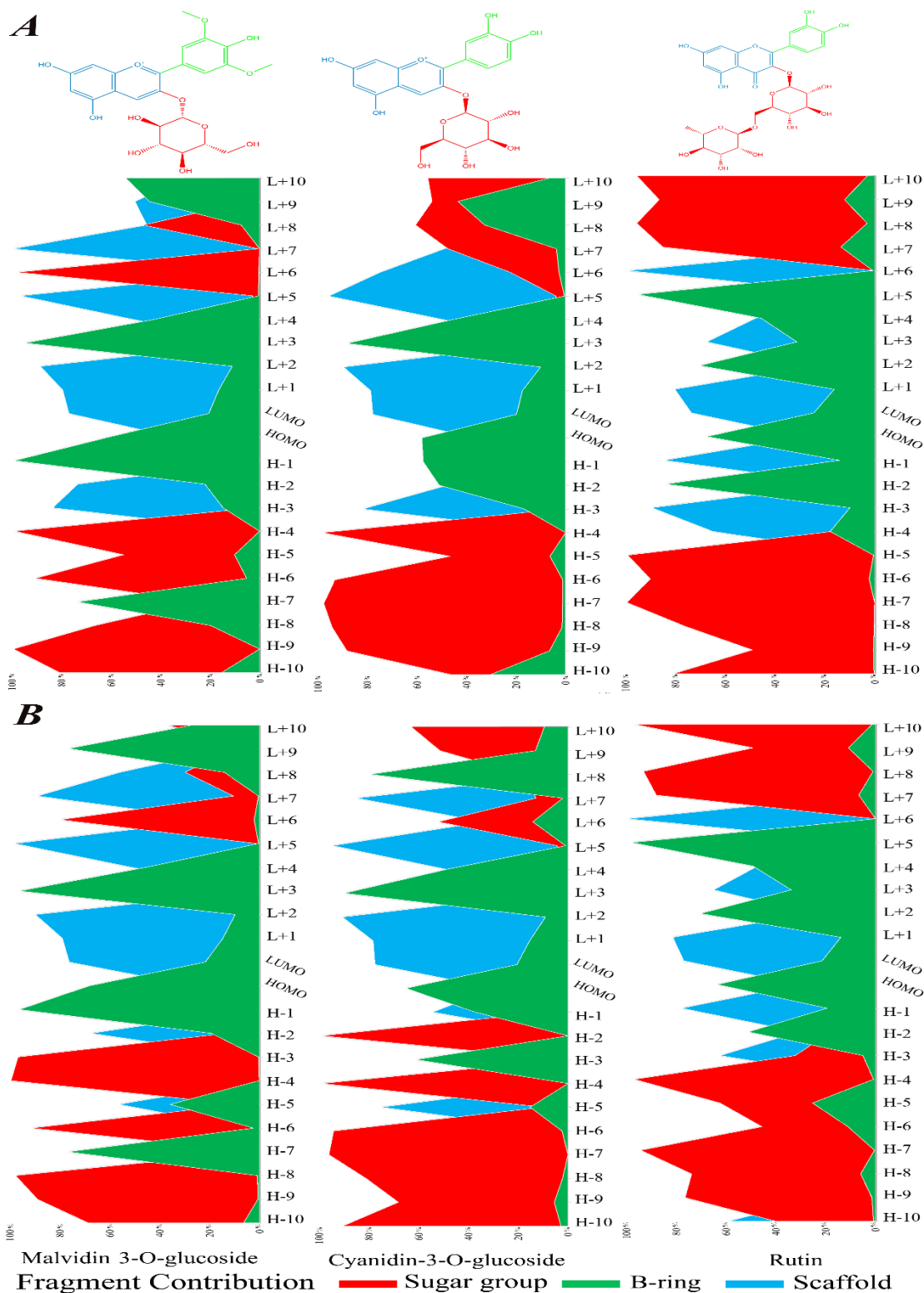
372

373 **Fig.6.** The calculated HOMO/LUMO and  $\Delta E_{gaps}$  for studied ligands at (A) HF and (B)  
 374 B3LYP methods. As shown, the chemical backbones of selected compounds display  
 375 significant variation in the distribution of frontier molecular orbitals and MEPs. This means  
 376 that the chemical nature of flavonoids backbone and its attached moieties have an impact on  
 377 the distribution of molecular orbitals. MEP surfaces show that dispersion of positive/negative  
 378 charges of ligand structures was partially different at recruited quantum methods. In each  
 379 MEP surface, red color represented the distribution of negative charges where the blue  
 380 functioned opposite. Indeed, the red zone is favorable for electrophilic attacks and vice versa.

381 Indeed, the results demonstrate that the chemical structure of rutin is harder than cyanidin-  
382 3-O-glucoside, and malvidin-3-O-glucoside (*Suppl. File S2- Table 1*). Additionally, these  
383 calculations to analyze of the electronic configuration of ligand-protein complex (in a sphere  
384 via 5 Å radius obtained from docking outputs), optimized free ligand and protein alone were  
385 displayed that the ligand-protein complex is harder than other free structures, and the  
386 hardness confirmed the deterrence (or absorption) of ligand against studied active sites  
387 (*Suppl. File S2- Table 1*). According to the HSAB concept, both “hard and soft” terms are  
388 applying for determining orbitals overlap to particular chemical cases, as addressed in the  
389 above-mentioned supplementary files. The application of the HSAB concept for prediction of  
390 inhibitor-target interactions is formerly documented to predict potential  
391 electrophilic/nucleophilic attacks within target active sites (LoPachin *et al.*, 2012). In this  
392 regard, the studied compounds displayed different chemical hardness/softness values by  
393 which such features may determine the effectiveness of their backbone to correctly interact  
394 with a set of catalytic/binding residues in the active site of target enzymes.

395  
396 The results of the electronic structures also revealed that the sugar moiety displayed a  
397 weak role in the contribution of molecular orbitals (around HOMO and LUMO), thereby, it  
398 functions as a donor group in the structure of ligands (*Fig.7*). For this fragment, the highest  
399 contribution in *HOMO -3* (for C3G and M3G) and *HOMO -4* (for rutin) orbitals were  
400 observed while it showed the lowest participation in *empty LUMO* and *LUMO -6* orbitals.  
401 However, this data speculates that the sugar group may participate in the distribution of  
402 molecular orbitals of protein (*LUMO* and *higher LUMO*). Indeed, the data of *LUMO* and  
403 higher *LUMO* orbitals has suggested that the participation of active site residues in the  
404 *LUMO* orbitals determined the type of interaction (*i.e.*, soft-soft or hard-hard) and the kind of  
405 control (*i.e.*, frontier and charge controlled). In summary, the computational results of  
406 quantum chemical evaluations demonstrate the importance of molecular orbitals distribution  
407 in the structure of ligands, which affected by the presence of sugar moiety, played a  
408 significant function in the interaction of ligands or their substructures with active site  
409 residues.





410

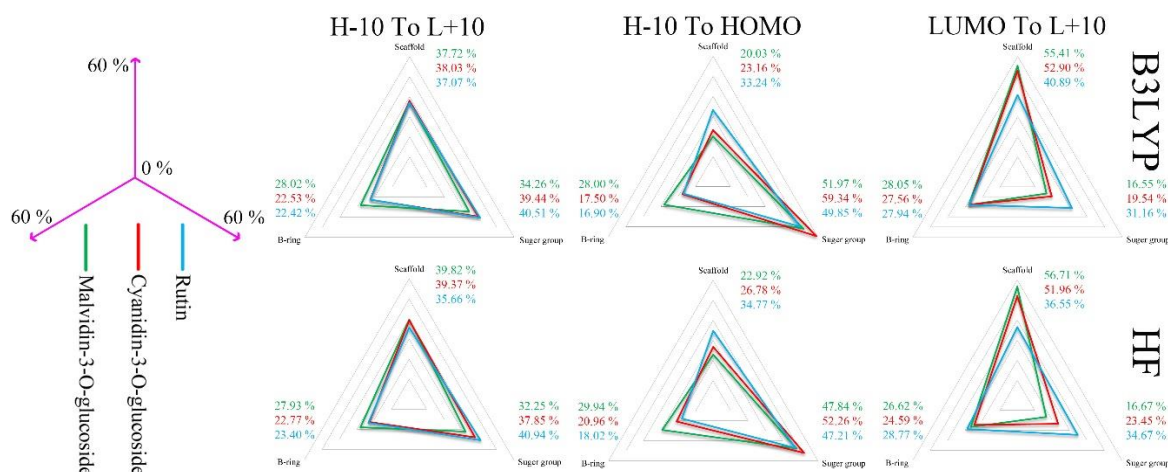
411 **Fig.7.** The role of studied fragments in the distribution of MOs at (A) HF and (B) B3LYP  
 412 methods. The B-ring fragment showed maximum participation in the distribution of HOMO  
 413 orbital and acts as a donor group. Also, the A/C rings scaffold fragment (blue color)  
 414 displayed higher participation in LUMO orbital and functions as an acceptor group.

415

416

417 **3.5. STRUCTURE-ACTIVITY RELATIONSHIPS**

418 As detailed in **Fig.8**, the sugar fragment has a high chance to interact with a variety of  
 419 peripheral, inner/outer residues of studied active sites in comparison to B-ring and A/C  
 420 scaffold fragments. Applying occupied (HOMO and *lower HOMO*) and unoccupied (LUMO  
 421 and *higher LUMO*) orbitals to investigate the role of ligand substructures in the distribution  
 422 of molecular orbitals revealed that the sugar moiety of the studied ligands has a highest  
 423 distribution in the molecular orbitals (HOMO to *HOMO -10*); consequently, this functional  
 424 chemical group is able to transfer electron to the side of unoccupied orbitals in protein active  
 425 site. Similarly, the scaffold fragment shared maximum involvement in the distribution of  
 426 unoccupied orbitals, chemically could receive electron from protein.  
 427



428 **Fig.8.** The total percentage of MO distributions of studied fragments including B-ring,  
 429 sugar moiety and A/C rings of backbone scaffold. The numerical values indicated the portion  
 430 of each moiety in the distribution of MOs. The maximum percentage of calculated MOs for  
 431 each compound shown in green, blue and red colors.  
 432  
 433

434 **4. DISCUSSION**

435 Various reports confirmed the neuroprotective effect of flavonoids. Rivera *et al.* (Rivera *et al.*  
 436 *et al.*, 2004) reported that the neuroprotective effect of flavonoids is associated with their  
 437 chemical structures (Rivera *et al.*, 2004). Das *et al.* (Das *et al.*, 2017) computationally  
 438 investigated the anti-Alzheimer activity of several flavonoids against AChE enzyme and  
 439 nominated some of them as possible targets for further studies. Other studies (Trebaticka and  
 440 Ďuračková, 2015) also reviewed the health benefits of polyphenols against metal disorders  
 441 and suggested that these compounds are valuable natural medications to alleviate the  
 442 oxidative stress of neurodegenerative diseases. Similarly, Ayaz *et al.* (Ayaz *et al.*, 2019)  
 443 addressed the effectiveness of flavonoids as potent biomolecules in the hallmark of aging and  
 444 other neurological disorders prevention.

445 In the wake of docking simulation drawbacks, researches have been documented that most  
 446 of docking limitations are owing to the lack of accurate scoring function to highlight the  
 447 essence of protein-ligand interactions at atomistic levels (Kokubo *et al.*, 2013). Available  
 448 algorithms, despite their popularity, may not wholly meet up the requirements for showing  
 449 how ligands substructures, functional groups or central backbone atoms might change  
 450 pouring of electron flow into protein active site cavity (Raha and Merz, 2004, Rasouli *et al.*,  
 451 2017).

452 The information of interacted ligand-protein complex helps researchers to understand  
453 physical behavior, which means visible interaction of ligand-protein complex, of ligands after  
454 gluing to their target residues. Accordingly, the functional roles of active site associated  
455 chemical additions such as water molecules or ions have widely been ruled out by docking  
456 simulation tools because there has rarely been a proper scoring model to explicit the behavior  
457 of these chemical molecules during ligand-protein interlinkage (Kokubo *et al.*, 2013).

458 For instance, the results demonstrated that Mg ion of GSK3 $\beta$  active site participated in the  
459 distribution of MOs at both methods, formed H-bonds with the side chain of docked ligands  
460 while docking outcomes only highlighted its role for interaction with two ligands. Therefore,  
461 docking scoring problems loom large when virtual screening pipelines applied such scoring  
462 functions or predictive models to filter and screen top hits of large drug-like libraries for  
463 further pharmaceutical application (Korb *et al.*, 2012, Raha and Merz, 2004).

464 Previously, studies revealed that coupling quantum-based data with docking results could  
465 provide new structural insight into binding mode of phenolic compounds and carbohydrate  
466 digestive enzymes (Rasouli *et al.*, 2017). Discrimination of top docked ligands by  
467 considering both docking binding energies and distribution of FMOs can help researchers to  
468 interpret docking results accurately. Other studies (Wasukan *et al.*, 2019) reported that  
469 combining QM calculations and docking results provided deeper understanding of silver  
470 nanoparticle-mediated cytochrome P450 inhibition. More interestingly, Lukac *et al.* (Lukac *et al.*,  
471 2019) have shown that the combination of QM outcomes with calculated or predicted  
472 LogP values was a reliable approach to improve the accuracy of protein-ligand binding  
473 energies. Very recently, researchers (Cavasotto *et al.*, 2018) reviewed the importance and  
474 functionality of QM-based calculations in protein-ligand docking and reported that these  
475 methods could provide invaluable information about the chemical basis of protein-ligand  
476 interactions at atomistic levels.

477 Although QM analyses were applied to improve of protein-ligand binding energies  
478 calculations, two problems including *cost of computation time/hardware for each step of QM*  
479 *analysis* (Raha and Merz, 2004) and *general uncertainty of docking scoring functions* limited  
480 large-scale utilizations of these methods to screen millions of chemical compounds  
481 (Cavasotto *et al.*, 2018). Indeed, the current literature does not investigate the simultaneous  
482 distribution of quantum MOs throughout ligand backbone and active site cavity at different  
483 levels, instead inserting greater emphasis on small molecule inhibitors after interaction with  
484 protein amino acids. However, this data was displayed that a possible change in the numerical  
485 values of quantum MOs is associated with both substitution of ligand backbone functional  
486 groups and specificity of active site amino acids side chains. Additionally, at two studied QM  
487 methods, ligands and the nearby amino acids showed their contribution to share favorable  
488 MOs by which the portion of most important studied fragments judged. At all, quantum  
489 chemical analysis is a trustworthy approach to study a variety of chemical reactions, chemical  
490 bonds (Ghafari and Gholipour, 2015, Jooneghani and Gholipour, 2019, Solimannejad and  
491 Ghafari, 2013) and other features related to both ligands and receptors to provide new  
492 structural insights into molecular interaction of inhibitors and potential active sites.

493 Findings suggest that the chemical modification of flavonoids skeleton determined the  
494 effectiveness of these ligands to interact with target amino acids. The structural variability of  
495 flavonoids is thought to be a valuable potency to alter the normal function of their targets by  
496 providing dose-dependent inhibitory properties (Rasouli *et al.*, 2017, Rasouli *et al.*, 2018,  
497 Rasouli *et al.*, 2018). It seems obvious that the variation and/or the alternation of attached –  
498 OH groups to flavonoid backbones (at B/C-rings and C2=C3 positions) could change their  
499 toxicity effect against the aggregation of A $\beta$  (Lee *et al.*, 2016). Also, other researchers have  
500 been documented that the biological activity of flavonoids is directly associated with the  
501 variability of their chemical structure (Rasouli *et al.*, 2018, Xiao, 2017). The B-ring of rutin,

502 C3G and M3G have different numbers of –OH groups and C3G and M3G have the same  
503 sugar group at the C2=C3 position, while rutin has two sugar units in this position. Thus,  
504 these chemical substitutions will effectively modify the tendency of these ligands to bind to  
505 active site amino acids.

506 Other investigations also suggest that the acetylation of flavonoids backbone at different  
507 positions may change the biological functionality of these metabolites (Chebil *et al.*, 2007).  
508 Interestingly, the antioxidant activity of flavonoids is directly linked to the number of  
509 attached –OH groups to their central skeleton and without these chemical moieties are not  
510 able to affect cellular signaling pathways (Chen *et al.*, 2017). The growing body of evidence  
511 also speculates that antioxidant and the inhibitory profile of some flavonoid compounds  
512 against protein kinase C $\delta$  receptor are correlated with the number of B-ring hydroxyl groups  
513 (Kongpichitchoke *et al.*, 2015). Generally, different factors such as hydroxylation,  
514 methylation, C2=C3 double bond, the –OH linked to the C3 position, glycosylation,  
515 acetylation and the number of –OH groups are caused various modifications in flavonoids  
516 backbones and changed their biological behavior within the cell (Xiao, 2017).

517 As a biological standpoint, targeting  $\tau$  protein kinases using small molecule inhibitors  
518 should consider a list of pros and cons to overcome the available challenges with current  
519 strategies to design anti-Alzheimer drugs (Chico *et al.*, 2009, Martin *et al.*, 2013). An  
520 important point should be addressed is that bioavailability and pharmacokinetics of drug-like  
521 compounds will define their functional inhibitory properties because most of these  
522 compounds are not reached CNS *in vivo* (Trebaticka and Ďuračková, 2015). More  
523 importantly, computational analyses only displayed how do active site residues selectively (or  
524 randomly) interact with a variety of chemical substances (Ghazvini *et al.*, 2018, Rasouli *et al.*,  
525 2017), and these outcomes are effective whenever clinical intervention studies approve  
526 the quality of natural products for alleviating human diseases (Yella *et al.*, 2018).

527 Recommending natural products as promising medications for the treatment of human  
528 diseases is not a primitive strategy and this is mainly ascribed to considerable numbers of  
529 biological factors (*e.g.* genetic factors, body metabolism, biological barriers, plasma proteins,  
530 target resistance, active site mutations, reactivity of structural moieties, instability, low  
531 solubility, immunological responses, interaction with other cellular targets, violation from  
532 filtering systems such as *Lipinski Rule of Five*, *etc.*) may simply change the expected  
533 biological properties of natural ligands (Amirkia and Heinrich, 2014, Press *et al.*, 2019).  
534 Specification of flavonoids backbones to interact with a variety of protein kinases by  
535 improving flavonoids selectivity and affinity, bioavailability, metabolism and designing  
536 future smart flavonoids using coupling advanced chemical computations and *in vivo* studies  
537 will decrease the number of clinical failures and improve the applicability of introduced  
538 compounds for AD prevention. By and large, greater focuses should be inserted on the  
539 transportability through physical barriers and metabolism of newly designed drugs within the  
540 body for long-term clinical success against AD (Chico *et al.*, 2009).

541 The outcomes represented that in addition to docking physical interactions, other chemical  
542 influential forces such as distribution of MOs between active site residues and chemical  
543 moieties of ligands (or their substructures) determine the “*type of interaction*” between  
544 ligands and receptors. As shown, molecular orbitals are quintessential parts of each chemical  
545 interaction, and considering their functional roles for expansion drug-like scaffolds may  
546 lower the total yield of virtual screening outcomes but produce promising backbones for  
547 further studies. Developing MOs descriptors using huge chemical libraries is highly  
548 recommended and such outputs will provide valuable treasures of quantum data for  
549 interpretation and filtering of virtual screening results. The simultaneous application of  
550 docking and QCAs coupled with other high-quality *in silico* methods such as molecular  
551 dynamic simulation, machine learning, data-mining, and QSAR validations might offer an

552 unprecedented opportunity to highlight all possible anti-Alzheimer drug-like candidates by  
553 applying heterogeneous datasets generated from these methods.

#### 554 **5. CONCLUDING REMARKS**

555 The results herein showed that flavonoids metabolites might interact with brain protein  
556 kinases but the variation of their backbone would lead to an increase or decrease in their  
557 binding energies. The outcomes were also shown that some flavonoid metabolites could  
558 interact with more than two kinases; therefore, these ingredients might have several targets  
559 within the brain. Interestingly, coupling chemical quantum analysis with docking results  
560 highlighted the functional roles of molecular orbital distribution between ligands and  
561 receptors in the determinations of possible interactions among studied complexes. The overall  
562 finding from this research may be widely applicable for drug design experts in the extraction  
563 of molecular mode of action of flavonoids using coupling advanced computational methods  
564 with available methods. Whether this premise is true or not, further development of this  
565 finding to approve its efficacy is strongly acknowledged.

#### 567 **CONFLICT OF INTEREST**

568 The authors declare no competing financial interest.

569

#### 570 **ACKNOWLEDGMENT**

571 None.

572

#### 573 **REFERENCES**

574 Adler, Paula, Mayne, Janice, Walker, Krystal, Ning, Zhibin, Figeys, Daniel. Therapeutic targeting of  
575 casein kinase 1 $\delta/\epsilon$  in an Alzheimer's disease mouse model. *J. Proteome Res.* 18(9) (2019) 3383-  
576 3393. DOI: <https://doi.org/10.1021/acs.jproteome.9b00312>

577 Ahn, Jae Suk, Radhakrishnan, Mala L, Mapelli, Marina, Choi, Sungwoon, Tidor, Bruce, Cuny, Gregory  
578 D, Musacchio, Andrea, Yeh, Li-An, Kosik, Kenneth S. Defining Cdk5 ligand chemical space with small  
579 molecule inhibitors of tau phosphorylation. *Chem Biol.* 12(7) (2005) 811-823. DOI:  
580 10.1016/j.chembiol.2005.05.011

581 Alvarez, Alejandra, Toro, Rodrigo, Cáceres, Alfredo, Maccioni, Ricardo B. Inhibition of tau  
582 phosphorylating protein kinase cdk5 prevents  $\beta$ -amyloid-induced neuronal death. *FEBS Lett.* 459(3)  
583 (1999) 421-426. DOI: 10.1016/s0014-5793(99)01279-x

584 Amirkia, Vafa, Heinrich, Michael. Alkaloids as drug leads—A predictive structural and biodiversity-  
585 based analysis. *Phytochem. Lett.* 10 (2014) xlviii-lviii. DOI:  
586 <https://doi.org/10.1016/j.phytol.2014.06.015>

587 Aoki, Masaaki, Yokota, Takehiro, Sugiura, Ikuko, Sasaki, Chizuko, Hasegawa, Tsukasa, Okumura,  
588 Chieko, Ishiguro, Koichi, Kohno, Toshiyuki, Sugio, Shigetoshi, Matsuzaki, Takao. Structural insight into  
589 nucleotide recognition in tau-protein kinase I/glycogen synthase kinase 3 $\beta$ . *Acta Crystallogr D Biol*  
590 *Crystallogr.* 60(3) (2004) 439-446. DOI: 10.1107/S090744490302938X

591 Association, Alzheimer's. 2018 Alzheimer's disease facts and figures. *Alzheimers Dement* 14(3)  
592 (2018) 367-429. DOI: <https://doi.org/10.1016/j.jalz.2018.02.001>

593 Ayaz, Muhammad, Sadiq, Abdul, Junaid, Muhammad, Ullah, Farhat, Ovais, Muhammad, Ullah, Ikram,  
594 Ahmed, Jawad, Shahid, Muhammad. Flavonoids as prospective neuroprotectants and their  
595 therapeutic propensity in aging associated neurological disorders. *Front. Aging Neurosci.* 11 (2019)  
596 1-15. DOI: <https://doi.org/10.3389/fnagi.2019.00155>

597 Bietz, Stefan, Urbaczek, Sascha, Schulz, Benjamin, Rarey, Matthias. Protoss: a holistic approach to  
598 predict tautomers and protonation states in protein-ligand complexes. *J Cheminform.* 6(1) (2014)  
599 12-16. DOI: 10.1186/1758-2946-6-12



600 Cavasotto, Claudio N, Adler, Natalia S, Aucar, Maria G. Quantum chemical approaches in structure-  
601 based virtual screening and lead optimization. *Front. Chem.* 6 (2018) 188-191. DOI:  
602 <https://doi.org/10.3389/fchem.2018.00188>

603 Chebil, Latifa, Anthoni, Julie, Humeau, Catherine, Gerardin, Christine, Engasser, Jean-Marc, Ghoul,  
604 Mohamed. Enzymatic acylation of flavonoids: Effect of the nature of the substrate, origin of lipase,  
605 and operating conditions on conversion yield and regioselectivity. *J Agric Food Chem* 55(23) (2007)  
606 9496-9502. DOI: 10.1021/jf071943j

607 Chen, Lei, Teng, Hui, Jia, Zhen, Battino, Maurizio, Miron, Anca, Yu, Zhiling, Cao, Hui, Xiao, Jianbo.  
608 Intracellular signaling pathways of inflammation modulated by dietary flavonoids: The most recent  
609 evidence. *Crit Rev Food Sci Nutr* (2017) 1-17. DOI: 10.1080/10408398.2017.1345853

610 Chico, Laura K, Van Eldik, Linda J, Watterson, D Martin. Targeting protein kinases in central nervous  
611 system disorders. *Nat. Rev. Drug Discov.* 8(11) (2009) 892-909. DOI:10.1038/nrd2999

612 Clark, EA, Leach, KL, Trojanowski, JQ, Lee, VM. Characterization and differential distribution of the  
613 three major human protein kinase C isozymes (PKC alpha, PKC beta, and PKC gamma) of the central  
614 nervous system in normal and Alzheimer's disease brains. *Lab Invest.* 64(1) (1991) 35-44. PMID:  
615 1990207

616 da Silva, Rodrigo R, Ramalho, Teodorico C, Santos, Joana M, Figueroa-Villar, J Daniel. On the limits of  
617 highest-occupied molecular orbital driven reactions: the frontier effective-for-reaction molecular  
618 orbital concept. *J Phys Chem A* 110(3) (2006) 1031-1040. DOI: 10.1021/jp054434y

619 Das, Subrata, Laskar, Monjur A, Sarker, Satyajit D, Choudhury, Manabendra D, Choudhury, Prakash  
620 Roy, Mitra, Abhijit, Jamil, Shajarahtunnur, Lathiff, Siti Mariam A, Abdullah, Siti Awanis, Basar,  
621 Norazah. Prediction of Anti-Alzheimer's Activity of Flavonoids Targeting Acetylcholinesterase in  
622 silico. *Phytochem Anal* 28(4) (2017) 324-331. DOI: 10.1002/pca.2679

623 Dolan, Philip J, Johnson, Gail VW. The role of tau kinases in Alzheimer's disease. *Curr Opin Drug*  
624 *Discov Devel* 13(5) (2010) 595-603. PMID: PMC2941661

625 Dubois, Bruno, Epelbaum, Stephane, Nyasse, Francis, Bakardjian, Hovagim, Gagliardi, Geoffroy,  
626 Uspenskaya, Olga, Houot, Marion, Lista, Simone, Cacciamani, Federica, Potier, Marie-Claude.  
627 Cognitive and neuroimaging features and brain  $\beta$ -amyloidosis in individuals at risk of Alzheimer's  
628 disease (INSIGHT-preAD): a longitudinal observational study. *Lancet Neurol* 17(4) (2018) 335-346.  
629 DOI: 10.1016/S1474-4422(18)30029-2

630 Faria, Ana, Mateus, Nuno, Calhau, Conceição. Flavonoid transport across blood-brain barrier:  
631 Implication for their direct neuroprotective actions. *Nutr Aging* 1(2) (2012) 89-97. DOI:  
632 10.3233/NUA-2012-0005

633 Faria, Ana, Meireles, Manuela, Fernandes, Iva, Santos-Buelga, Celestino, Gonzalez-Manzano, Susana,  
634 Dueñas, Montserrat, de Freitas, Victor, Mateus, Nuno, Calhau, Conceição. Flavonoid metabolites  
635 transport across a human BBB model. *Food Chem* 149 (2014) 190-196. DOI:  
636 10.1016/j.foodchem.2013.10.095

637 Faria, Ana, Pestana, Diogo, Teixeira, Diana, Azevedo, Joana, Freitas, Victor, Mateus, Nuno, Calhau,  
638 Conceição. Flavonoid transport across RBE4 cells: a blood-brain barrier model. *Cell Mol Biol Lett*  
639 15(2) (2010) 234-241. DOI: 10.2478/s11658-010-0006-4

640 Ferri, Paola, Angelino, Donato, Gennari, Lorenzo, Benedetti, Serena, Ambrogini, Patrizia, Del Grande,  
641 Paolo, Ninfali, Paolino. Enhancement of flavonoid ability to cross the blood-brain barrier of rats by  
642 co-administration with  $\alpha$ -tocopherol. *Food Funct.* 6(2) (2015) 394-400. DOI: 10.1039/c4fo00817k

643 Frisch, MJ, Trucks, GW, Schlegel, HB, Scuseria, GE, Robb, MA, Cheeseman, JR, Montgomery Jr, JA,  
644 Vreven, TTKN, Kudin, KN, Burant, JC. Gaussian 03, revision C. 02; Gaussian, Inc. *Wallingford, CT* 26  
645 (2004).

646 Fukui, Kenichi, Yonezawa, Teijiro, Nagata, Chikayoshi, Shingu, Haruo. Molecular orbital theory of  
647 orientation in aromatic, heteroaromatic, and other conjugated molecules. *J Chem Phys* 22(8) (1954)  
648 1433-1442.

649 Fukui, Kenichi, Yonezawa, Teijiro, Shingu, Haruo. A molecular orbital theory of reactivity in aromatic  
650 hydrocarbons. *J Chem Phys* 20(4) (1952) 722-725.

651 Ghafari, Saber, Gholipour, Alireza. Simultaneous interactions of pyrimidine ring with BeF<sub>2</sub> and BF<sub>3</sub>  
652 in BeF<sub>2</sub>···X-Pyr···BF<sub>3</sub> complexes: non-cooperativity. *J. Mol. Model.* 21(10) (2015) 1-7. DOI:  
653 <https://doi.org/10.1007/s00894-015-2795-x>

654 Ghazvini, Seyed Mohammad Bagher Hosseini, Safari, Parvin, Mobinikhaledi, Akbar, Moghanian,  
655 Hassan, Rasouli, Hassan. Synthesis, characterization, anti-diabetic potential and DFT studies of 7-  
656 hydroxy-4-methyl-2-oxo-2H-chromene-8-carbaldehyde oxime. *Spectrochim Acta A Mol Biomol*  
657 *Spectrosc.* 205 (2018) 111-131. DOI: 10.1016/j.saa.2018.07.009

658 Glaab, Enrico. Building a virtual ligand screening pipeline using free software: a survey. *Brief*  
659 *Bioinform* 17(2) (2015) 352-366. DOI: 10.1093/bib/bbv037

660 Griffin, Rebecca J, Moloney, Aileen, Kelliher, Mary, Johnston, Janet A, Ravid, Rivka, Dockery, Peter,  
661 O'connor, Rosemary, O'Neill, Cora. Activation of Akt/PKB, increased phosphorylation of Akt  
662 substrates and loss and altered distribution of Akt and PTEN are features of Alzheimer's disease  
663 pathology. *J Neurochem* 93(1) (2005) 105-117. DOI: 10.1111/j.1471-4159.2004.02949.x

664 Hoffmann, Roald, Woodward, RB. Orbital symmetries and endo-exo relationships in concerted  
665 cycloaddition reactions. *J. Am. Chem. Soc.* 87(19) (1965) 4388-4389. DOI:  
666 <https://doi.org/10.1021/ja00947a033>

667 Hoffmann, Roald, Woodward, Robert B. Conservation of orbital symmetry. *Acc. Chem. Res* 1(1)  
668 (1968) 17-22. DOI; <https://doi.org/10.1002/anie.196907811>

669 Jooneghani, Saber Ghafari Nikoo, Gholipour, Alireza. Mutual cooperation of  $\pi$ - $\pi$  stacking and  
670 pnictogen bond interactions of substituted monomeric Lawesson's reagent and pyridine rings:  
671 Theoretical insight into Pyr||X-PhPS<sub>2</sub>⊥pyr complexes. *Chem. Phys. Lett* 721 (2019) 91-98. DOI:  
672 <https://doi.org/10.1016/j.cplett.2019.02.027>

673 Klebe, Gerhard. Virtual ligand screening: strategies, perspectives and limitations. *Drug Discov. Today*  
674 11(13-14) (2006) 580-594. DOI:10.1016/j.drudis.2006.05.012

675 Klopman, Gilles. Chemical reactivity and the concept of charge-and frontier-controlled reactions. *J.*  
676 *Am. Chem. Soc.* 90(2) (1968) 223-234. DOI: <https://doi.org/10.1021/ja01004a002>

677 Kokubo, Hironori, Tanaka, Toshimasa, Okamoto, Yuko. Prediction of protein-ligand binding  
678 structures by replica-exchange umbrella sampling simulations: application to kinase systems. *J.*  
679 *Chem. Theory Comput* 9(10) (2013) 4660-4671. DOI: dx.doi.org/10.1021/ct4004383

680 Kongpichitchoke, Teeradate, Hsu, Jue-Liang, Huang, Tzou-Chi. Number of hydroxyl groups on the B-  
681 ring of flavonoids affects their antioxidant activity and interaction with phorbol ester binding site of  
682 PKC $\delta$  C1B domain: in vitro and in silico studies. *J Agric Food Chem* 63(18) (2015) 4580-4586. DOI:  
683 10.1021/acs.jafc.5b00312

684 Korb, Oliver, Olsson, Tjelvar SG, Bowden, Simon J, Hall, Richard J, Verdonk, Marcel L, Liebeschuetz,  
685 John W, Cole, Jason C. Potential and limitations of ensemble docking. *J. Chem. Inf. Model.* 52(5)  
686 (2012) 1262-1274. DOI: dx.doi.org/10.1021/ci2005934

687 Lee, Hyuck Jin, Kerr, Richard A, Korshavn, Kyle J, Lee, Jeeyeon, Kang, Juhye, Ramamoorthy,  
688 Ayyalusamy, Ruotolo, Brandon T, Lim, Mi Hee. Effects of hydroxyl group variations on a flavonoid  
689 backbone toward modulation of metal-free and metal-induced amyloid- $\beta$  aggregation. *Inorg. Chem.*  
690 *Front.*, 3(3) (2016) 381-392. DOI: 10.1039/C5QI00219B

691 Lescot, Elodie, Bureau, Ronan, Sopkova-de Oliveira Santos, Jana, Rochais, Christophe, Lisowski,  
692 Vincent, Lancelot, Jean-Charles, Rault, Sylvain. 3D-QSAR and docking studies of selective GSK-3 $\beta$   
693 inhibitors. Comparison with a thieno [2, 3-b] pyrrolizinone derivative, a new potential lead for GSK-  
694 3 $\beta$  ligands. *J. Chem. Inf. Model.* 45(3) (2005) 708-715. DOI: <https://doi.org/10.1021/ci050008y>

695 Liu, Shu-Lei, Wang, Chong, Jiang, Teng, Tan, Lan, Xing, Ang, Yu, Jin-Tai. The role of Cdk5 in  
696 Alzheimer's disease. *Mol Neurobiol* 53(7) (2016) 4328-4342. DOI: 10.1007/s12035-015-9369-x

697 Llorens-Marín, María, Jurado, Jerónimo, Hernández, Félix, Ávila, Jesús. GSK-3 $\beta$ , a pivotal kinase in  
698 Alzheimer disease. *Front Mol Neurosci* 7 (2014) 46. DOI: <https://doi.org/10.3389/fnmol.2014.00046>

699 Long, Alexander, Zhao, Huilin, Huang, Xin. Structural basis for the interaction between casein kinase  
700 1 delta and a potent and selective inhibitor. *J Med Chem.* 55(2) (2012) 956-960. DOI:  
701 10.1021/jm201387s

702 LoPachin, Richard M, Gavin, Terrence, DeCaprio, Anthony, Barber, David S. Application of the hard  
703 and soft, acids and bases (HSAB) theory to toxicant–target interactions. *Chem. Res. Toxicol.* 25(2)  
704 (2012) 239-251. DOI: <https://doi.org/10.1021/tx2003257>  
705 Lu, Tian, Chen, Feiwu. Multiwfn: a multifunctional wavefunction analyzer. *J Comput Chem.* 33(5)  
706 (2012) 580-592. DOI: 10.1002/jcc.22885  
707 Lukac, Iva, Abdelhakim, Hend, Ward, Richard A, St-Gallay, Stephen A, Madden, Judith C, Leach,  
708 Andrew G. Predicting protein–ligand binding affinity and correcting crystal structures with quantum  
709 mechanical calculations: lactate dehydrogenase A. *Chem. Sci.* 10(7) (2019) 2218-2227. DOI:  
710 10.1039/C8SC04564J  
711 Maksić, Zvonimir B, Vianello, Robert. Comment on the paper “on the limits of highest-occupied  
712 molecular orbital driven reactions: the frontier effective-for-reaction molecular orbital concept”. *J.*  
713 *Phys. Chem. A* 110(36) (2006) 10651-10652. DOI: <https://doi.org/10.1021/jp061030c>  
714 Martin, Ludovic, Latypova, Xenia, Wilson, Cornelia M, Magnaudeix, Amandine, Perrin, Marie-Laure,  
715 Yardin, Catherine, Terro, Faraj. Tau protein kinases: involvement in Alzheimer's disease. *Ageing Res.*  
716 *Rev.* 12(1) (2013) 289-309. DOI: <http://dx.doi.org/10.1016/j.arr.2012.06.003>  
717 Maurer, Konrad, Volk, Stephan, Gerbaldo, Hector. Auguste D and Alzheimer's disease. *Lacent*  
718 349(9064) (1997) 1546-1549. DOI:[https://doi.org/10.1016/S0140-6736\(96\)10203-8](https://doi.org/10.1016/S0140-6736(96)10203-8)  
719 McDade, Eric, Bateman, Randall J. Stop Alzheimer's before it starts. *Nature* 547(7662) (2017) 153-  
720 155. DOI: 10.1038/547153a  
721 Ng, Yu Pong, Or, Terry Cho Tsun, Ip, Nancy Y. Plant alkaloids as drug leads for Alzheimer's disease.  
722 *Neurochem Int* 89 (2015) 260-270. DOI: 10.1016/j.neuint.2015.07.018  
723 Pearson, Ralph G. Hard and soft acids and bases. *J. Am. Chem. Soc.* 85(22) (1963) 3533-3539. DOI:  
724 <https://doi.org/10.1021/ja00905a001>  
725 Press, Neil J, Joly, Emilie, Ertl, Peter. Natural product drug delivery: A special challenge? , Progress in  
726 Medicinal Chemistry2019, pp. 157-187.  
727 Raha, Kaushik, Merz, Kenneth M. A quantum mechanics-based scoring function: study of zinc ion-  
728 mediated ligand binding. *J. Am. Chem. Soc.* 126(4) (2004) 1020-1021. DOI: 10.1021/ja038496i  
729 Ramalho, Teodorico C, Martins, Tales LC, Eduardo, Luiz, Borges, Pizarro, Figueroa-Villar, José Daniel.  
730 Influence of nonbonded interactions in the kinetics of formation of chalcogenol esters from  
731 chalcogenoacetylenes. *Int. J. Quantum Chem.* 95(3) (2003) 267-273. DOI:  
732 <https://doi.org/10.1002/qua.10680>  
733 Rasouli, Hassan, Hosseini-Ghazvini, Seyed Mohammad-Bagher, Adibi, Hadi, Khodarahmi, Reza.  
734 Differential  $\alpha$ -amylase/ $\alpha$ -glucosidase inhibitory activities of plant-derived phenolic compounds: a  
735 virtual screening perspective for the treatment of obesity and diabetes. *Food Funct.* 8(5) (2017)  
736 1942-1954. DOI: 10.1039/c7fo00220c  
737 Rasouli, Hassan, Hosseini-Ghazvini, Seyed Mohammad-Bagher, Khodarahmi, Reza. Therapeutic  
738 Potentials of the Most Studied Flavonoids: Highlighting Antibacterial and Antidiabetic  
739 Functionalities. *Studies in Natural Products Chemistry*, Elsevier2018, pp. 85-122.  
740 Rasouli, Hassan, Norooznehad, Amir Hossein, Rashidi, Tahereh, Hoseinkhani, Zohreh, Mahnam,  
741 Azadeh, Tarlan, Mitra, Moasefi, Narges, Mostafaei, Ali, Mansouri, Kamran. Comparative in  
742 vitro/theoretical studies on the anti-angiogenic activity of date pollen hydro-alcoholic extract:  
743 Highlighting the important roles of its hot polyphenols. *BiolImpacts* 8(4) (2018) 281–294. DOI:  
744 10.15171/bi.2018.31  
745 Rasouli, Hassan, Yarani, Reza, Pociot, Flemming, Popović-Djordjević, Jelena. Anti-diabetic potential of  
746 plant alkaloids: Revisiting current findings and future perspectives. *Pharmacol Res* 155 (2020)  
747 104723. DOI: <https://doi.org/10.1016/j.phrs.2020.104723>  
748 Rivera, Felicia, Urbanavicius, Jessika, Gervaz, Elena, Morquio, Andrea, Dajas, Federico. Some aspects  
749 of their vivo neuroprotective capacity of flavonoids: Bioavailability and structure-activity  
750 relationship. *Neurotox Res* 6(7-8) (2004) 543-553. PMID: 15639786

751 Schwab, Claudia, DeMaggio, Anthony J, Ghoshal, Nupur, Binder, Lester I, Kuret, Jeff, McGeer, Patrick  
752 L. Casein kinase 1 delta is associated with pathological accumulation of tau in several  
753 neurodegenerative diseases. *Neurobiol Aging* 21(4) (2000) 503-510. PMID: 10924763  
754 Scotti, Luciana, Scotti, Marcus T. In Silico Studies Applied to Natural Products with Potential Activity  
755 Against Alzheimer's Disease. Computational Modeling of Drugs Against Alzheimer's Disease,  
756 Springer2018, pp. 513-531.  
757 Shrestha, Sabina, Natarajan, Sathishkumar, Park, Ji-Hae, Lee, Dae-Young, Cho, Jin-Gyeong, Kim,  
758 Geum-Soog, Jeon, Yong-Jin, Yeon, Seung-Woo, Yang, Deok-Chun, Baek, Nam-In. Potential  
759 neuroprotective flavonoid-based inhibitors of CDK5/p25 from *Rhus parviflora*. *Bioorg Med Chem Lett*  
760 23(18) (2013) 5150-5154. DOI: <http://dx.doi.org/10.1016/j.bmcl.2013.07.020>  
761 Silva, Rodrigo R da, Santos, Joana M, Ramalho, Teodorico C, Figueroa-Villar, J Daniel. Concerning the  
762 FERMO concept and Pearson's Hard and Soft acid-base principle. *J. Braz. Chem. Soc.* 17(2) (2006)  
763 223-226. DOI: <http://dx.doi.org/10.1590/S0103-50532006000200002>  
764 Solimannejad, Mohammad, Ghafari, Saber. Ab initio study of ternary radical-molecule complexes  
765 between HCN (HNC) and HO (HS) species. *Struct. Chem.* 24(5) (2013) 1493-1498. DOI:  
766 <https://doi.org/10.1007/s11224-012-0184-y>  
767 Sun, Jing, Nan, Guangxian. The extracellular signal-regulated kinase 1/2 pathway in neurological  
768 diseases: A potential therapeutic target. *Int J Mol Med* 39(6) (2017) 1338-1346. DOI:  
769 10.3892/ijmm.2017.2962  
770 Sweeney, Melanie D, Sagare, Abhay P, Zlokovic, Berislav V. Blood-brain barrier breakdown in  
771 Alzheimer disease and other neurodegenerative disorders. *Nat Rev Neurol* 14(3) (2018) 133. DOI:  
772 10.1038/nrneurol.2017.188  
773 Tao, Peng, Schlegel, H Bernhard. A toolkit to assist ONIOM calculations. *J Comput Chem.* 31(12)  
774 (2010) 2363-2369. DOI: 10.1002/jcc.21524  
775 Tarricone, Cataldo, Dhavan, Rani, Peng, Junmin, Areces, Liliana B, Tsai, Li-Huei, Musacchio, Andrea.  
776 Structure and regulation of the CDK5-p25nck5a complex. *Mol. Cell* 8(3) (2001) 657-669. DOI:  
777 [https://doi.org/10.1016/S1097-2765\(01\)00343-4](https://doi.org/10.1016/S1097-2765(01)00343-4)  
778 Trebaticka, Jana, Ďuračková, Zdeňka. Psychiatric disorders and polyphenols: can they be helpful in  
779 therapy? *Oxid Med Cell Longev.* 2015 (2015) 248529. DOI: 10.1155/2015/248529  
780 Trott, Oleg, Olson, Arthur J. AutoDock Vina: improving the speed and accuracy of docking with a new  
781 scoring function, efficient optimization, and multithreading. *J Comput Chem* 31(2) (2010) 455-461.  
782 DOI: 10.1002/jcc.21334  
783 Wasukan, Nootcharin, Kuno, Mayuso, Maniratanachote, Rawiwan. Molecular docking as a promising  
784 predictive model for silver nanoparticle-mediated inhibition of cytochrome P450 enzymes. *J. Chem.*  
785 *Inf. Model.* 59 (2019) 5126-5134. DOI: <https://doi.org/10.1021/acs.jcim.9b00572>  
786 Wilkaniec, Anna, Czapski, Grzegorz A, Adamczyk, Agata. Cdk5 at crossroads of protein  
787 oligomerization in neurodegenerative diseases: facts and hypotheses. *J. Neurochem.* 136(2) (2016)  
788 222-233. DOI: <https://doi.org/10.1111/jnc.13365>  
789 Wilkaniec, Anna, Gąssowska-Dobrowolska, Magdalena, Strawski, Marcin, Adamczyk, Agata, Czapski,  
790 Grzegorz A. Inhibition of cyclin-dependent kinase 5 affects early neuroinflammatory signalling in  
791 murine model of amyloid beta toxicity. *J. Neuroinflammation* 15(1) (2018) 1-18. DOI  
792 10.1186/s12974-017-1027-y  
793 Xiao, Jianbo. Dietary flavonoid aglycones and their glycosides: Which show better biological  
794 significance? *Crit Rev Food Sci Nutr* 57(9) (2017) 1874-1905. DOI: 10.1080/10408398.2015.1032400  
795 Yang, Yuya, Bai, Lu, Li, Xiaorong, Xiong, Jie, Xu, Pinxiang, Guo, Chenyang, Xue, Ming. Transport of  
796 active flavonoids, based on cytotoxicity and lipophilicity: An evaluation using the blood-brain barrier  
797 cell and Caco-2 cell models. *Toxicol In Vitro.* 28(3) (2014) 388-396. DOI: 10.1016/j.tiv.2013.12.002  
798 Yella, Jaswanth, Yaddanapudi, Suryanarayana, Wang, Yunguan, Jegga, Anil. Changing trends in  
799 computational drug repositioning. *Pharmaceuticals* 11(2) (2018) 57-78. DOI:  
800 <http://dx.doi.org/10.3390/ph11020057>

801 Yuriev, Elizabeth, Ramsland, Paul A. Latest developments in molecular docking: 2010–2011 in  
802 review. *J Mol Recognit* 26(5) (2013) 215-239. DOI: 10.1002/jmr.2266

803

804

805

806

807